Journal of Solid State Chemistry **162,** 260–265 (2001)
doi:10.1006/jssc.2001.9285, available online at http://www.idealibrary.com on IDEAL®

Some Solid State Chemistry Aspects of Lead-Free Relaxor Ferroelectrics

J. Ravez and A. Simon[1]

ICMCB-CNRS, 87 avenue A. Schweitzer, 33608 Pessac, France

Published online August 22, 2001

IN HONOR OF PROFESSOR PAUL HAGENMULLER ON THE OCCASION OF HIS 80TH BIRTHDAY

Some solid state chemistry aspects are investigated in relaxor ferroelectrics of both perovskite and tetragonal tungsten bronze (TTB) structure. Various issues regarding composition, cationic charge, electronic configuration, and structure are discussed. The relaxor behavior appears when two different cations occupy the same crystallographic site. One of the cations in the octahedral site has to be ferroelectrically active. The relaxor effect is correlated to cationic distribution disorder in the same site, depending on composition and structure (perovskite or TTB).

Key Words: **lead-free; relaxor ferroelectrics; solid state chemistry.**

1. INTRODUCTION

Ferroelectric materials may be divided into two classes: classical ferroelectrics and relaxors (Table 1) (1). Typically, relaxors have at least one crystallographic site that is occupied by two or more ions. In addition to the usual applications for classical ferroelectrics, relaxors are of great interest for dielectrics in capacitors and actuators (2). Most relaxors are lead-based ceramics such as $PbMg_{1/3}Nb_{2/3}O_3$ (PMN) and derived compounds, or $Pb(M'_{1/2}M''_{1/2})O_3$ with long-range polar order. However, these compositions have the obvious disadvantages associated with the volatility and toxicity of PbO. Therefore, much current research is directed toward more environmentally friendly Pb-free relaxor materials.

To date, various physical models have been described to explain the properties of relaxors (3): compositional fluctuations and diffuse phase transition (4, 5), the superparaelectric model (6), the nanostructure-octahedral model (7 to 13), the dipole-glass or the more recent derived model (14, 15), the random-field model (16, 17), the domain-wall model (18), and the random-layer model (19, 20).

[1] To whom correspondence should be addressed. E-mail: simon@icmcb.u-bordeaux.fr. Fax: 33 05 56 84 27 61.

The present work discusses some of the solid state chemistry aspects of lead-free ferroelectric relaxors. The selected compositions belong to either perovskite or tetragonal tungsten bronze (TTB) families.

2. PEROVSKITE FERROELECTRIC RELAXORS DERIVED FROM $BaTiO_3$

2a. Results

Depending on both the substitution and the composition (Table 2), different types of behavior have been evidenced in binary systems (21):

— For homovalent substitutions in the M site (e.g., $Ba(Ti_{1-x}M_x)O_3$, $M = Zr, Sn, Ce$), the transition sequence was the same as that of $BaTiO_3$ for low values of x ($x \leq 0.10$, $M = Zr$). For greater values of x (e.g., $0.10 < x \leq 0.27$, $M = Zr$) there was only one rhombohedral, ferroelectric-$T_C \rightarrow$ cubic, paraelectric transition after the disappearance of the orthorhombic and tetragonal phases. For the highest values of x ($x > 0.27$, $M = Zr$) the behavior was of relaxor type. For example, Figs. 1 and 2 show the temperature dependences of both ε'_r and ε''_r for a ceramic with the composition $Ba(Ti_{0.65}Zr_{0.35})O_3$.

— For homovalent substitutions in both A and M sites (Table 2), the sequence was comparable to the previous one.

— For heterovalent substitutions in the A site (Table 2), the transition sequence was the same as that of $BaTiO_3$ up to relatively high temperatures of x ($x \leq 0.20$ for $Ba_{1-x}(La_{x/2}K_{x/2})TiO_3$). For higher values of x, a relaxor behavior was observed.

— For heterovalent substitutions in both A and M sites (Table 2) or in both M and X sites, the relaxor properties were observed from values of x as small as 0.05, i.e., for small substitution rates (22 to 25).

Relaxor composition regions were also obtained in various ternary diagrams. For example, Fig. 3 shows the results obtained in the $BaTiO_3$–$BaZrO_3$–$CaTiO_3$ ternary diagram: zone III presents a relaxor behavior. It is interesting to note that there is a ferroelectric–relaxor–paralectric phase transition sequence in the domain between zones II and III (21).

0022-4596/01 $35.00

TABLE 1
Some Physical Properties of Classical or Relaxor Ferroelectrics of Perovskite Type

	Classical ferroelectrics	Relaxors
Octahedral site occupation	—	More than one different cation
Composition heterogeneity	—	Nanoscopic scale
Polar region size	Microdomains	Nanodomains
Symmetry for $T \leq T_C$ (or T_m)	Tetragonal, orthorhombic, or rhombohedral	Macroscopically cubic (optical or X-ray diffraction studies)
Ferroelectric–paraelectric transition	Sharp	Diffuse
Frequency f dispersion of ε'_r or ε''_r for $T \leq T_C$ (or T_m)	ε'_r not dependent on f	ε'_r decreases when f increases
	ε''_r not dependent on f	ε''_r increases when f increases
Frequency dependence of T_C (or T_m)	T_C not dependent on f	T_m increases when f increases
Thermal variation of ε'_r in the paraelectric phase	Curie–Weiss law	Deviation from Curie–Weiss law
Thermal variation of P_s, at T_C (or T_m), on heating	Sharp (1st order trans.) or progressive (2nd order trans.) decrease at T_C; $P_s = 0$ if $T > T_C$	Progressive decrease with a polarization tail for $T \geq T_m$

T_C = ferroelectric Curie temperature; T_m = temperature of the maximum of permittivity ε'_r, for a relaxor; f = frequency; P_s = spontaneous polarization.

The main relaxor characteristics $\Delta T_m = T_m(10^5\ \text{Hz}) - T_m(10^2\ \text{Hz})$ and $\Delta\varepsilon'_r/\varepsilon'_r = [\varepsilon'_{r\,max.}(10^2\ \text{Hz}) - \varepsilon'_{r\,max.}(10^5\ \text{Hz})]/\varepsilon'_{r\,max.}$ (10^2 Hz) become higher as the composition deviates from $BaTiO_3$. Moreover, the composition range of solid solutions showing a relaxor behavior depends on the type of substitution. Table 3 gives comparative values of x for the same shift of T_m:

— For homovalent substitutions in the M site, the equal charge of the cations (e.g., Ti^{4+} and Zr^{4+}) requires a high substitution rate ($x = 0.35$).

— Coupled homovalent substitutions in both A and M sites generate higher heterogeneity leading to relatively lower values of x ($x = 0.225$).

— Concerning heterovalent substitutions only in the A site, the value of x is nevertheless high, because even for different charges, the relaxor effect is not enhanced by substitutions in such a site.

— For heterovalent substitutions in the M site, which are coupled of course with heterovalent ones in another site, the values of x are the lowest. This implies that the relaxor effect is mainly dependent on heterovalent substitutions in the M site.

In addition, the value of ΔT_m, which is a typical characteristic of the relaxor effect, was the highest for the limit composition of the solid solution $Ba_{1-x}Bi_{2x/3}TiO_3$ (Table 4). For example, Fig. 4 shows the result obtained for a ceramic with the composition $x = 0.15$. Indeed, although these compositions are lead-free, they contain Bi^{3+} which has a $6(sp)^2$ lone pair, like Pb^{2+}.

2b. Discussion

In perovskite-type compositions, the relaxor effect appears when at least two different cations occupy the same crystallographic site A or M. The more the substitution is in the M site, the greater is the effect. One of the two cations in

TABLE 2
Main Types of Lead-Free Solid Solutions and $BaTiO_2$ (BT)–Derived Domains

Substitution	Sites	Solid solutions and domains	Systems
Homovalent	M	$Ba(Ti_{1-x}M_x)O_3$ (M = Zr, Sn, Ce)	BT–$BaMO_3$
	A and M	$Ba_{1-x}Ca_x(Ti_{1-x}Zr_x)O_3$	BT–$CaZrO_3$
Heterovalent		$Ba_{1-x}K_{x/2}La_{x/2}TiO_3$	BT–"$K_{1/2}La_{1/2}TiO_3$"
	A	$Ba_{1-x}A_{2x/3}\square_{x/3}TiO_3$ (A = La, Bi)	BT–"$A_{2/3}TiO_3$"
		$Ba_{1-x/2}\square_{x/2}(Ti_{1-x}M_x)O_3$ (M = Nb, Ta)	BT–$Ba_{1/2}MO_3$
	A and M	$Ba_{1-x}K_x(Ti_{1-x}M_x)O_3$ (M = Nb, Ta)	BT–KMO_3
		$Ba_{1-x}Na_x(Ti_{1-x}Nb_x)O_3$	BT–$NaNbO_3$
	M and X	$Ba(Ti_{1-x}Li_x)O_{3-3x}F_{3x}$	BT–$BaLiF_3$
	A, M, and X	$Ba_{1-x}K_x(Ti_{1-x}Mg_x)O_{3-x}F_x$	BT–$KMgF_3$
		Various composition domains	BT–$BaZrO_3$–$CaTiO_3$ BT–$BaZrO_3$–$BaLiF_3$ BT–$BaZrO_3$–$CaLiF_3$ BT–$KNbO_3$–$CaTiO_3$

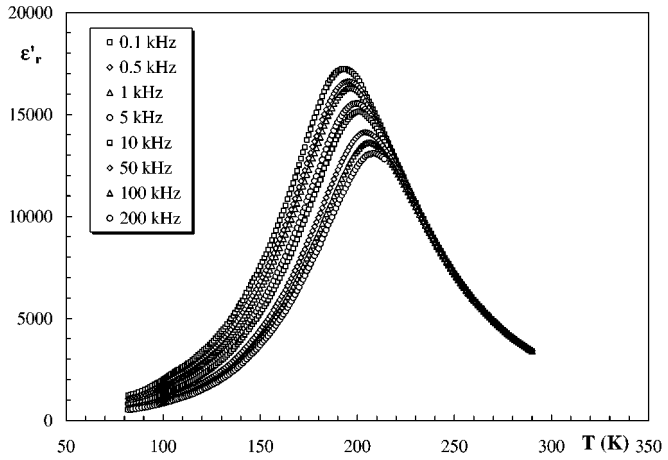

FIG. 1. Thermal variation of the real part of the permittivity ε'_r for a ceramic with composition $Ba(Ti_{0.65}Zr_{0.35})O_3$ (21).

this M site must be ferroelectrically active (for example Ti^{4+}, Nb^{5+}, or Ta^{5+}), so this cation is off-centered in the octahedral site and gives rise to a local dipolar moment.

In contrast to lead compositions, lead-free ones do not show ferroelectric properties when there is an order between the two atoms M' and M''; for barium compounds, the Ba^{2+} cation favors a long-range order (e.g., $BaSc_{1/2}Nb_{1/2}O_3$ or $BaMg_{1/3}Nb_{2/3}O_3$). In fact, lead-free relaxors derived from barium titanate are solid solutions. The substitution from the classical ferroelectric $BaTiO_3$ weakens the ferroelectric character (Ti^{4+} octahedral off-centered) and leads only to a local polarization. The two cations which occupy the same crystallographic site are not ordered.

Although the lead-free perovskite relaxors derived from $BaTiO_3$ are the most numerous, there are others, e.g., $Na_{1/2}Bi_{1/2}TiO_3$ (26).

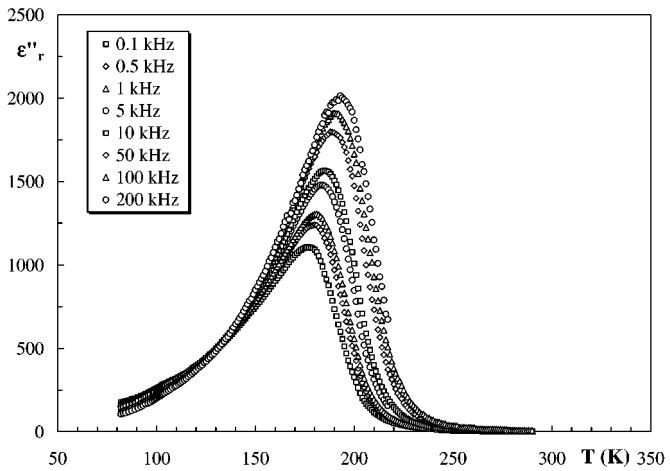

FIG. 2. Thermal variation of the imaginary part of the permittivity ε''_r for a ceramic with composition $Ba(Ti_{0.65}Zr_{0.35})O_3$ (21).

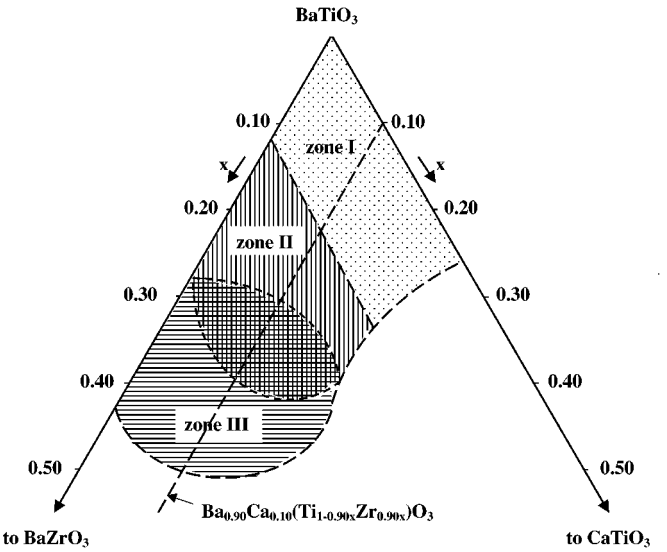

FIG. 3. Schematic representation of the $BaTiO_3$–$BaZrO_3$–$CaTiO_3$ ternary diagram (21).

3. LEAD-FREE TTB FERROELECTRIC RELAXORS

3a. Results

Figure 5 shows a schematic representation of the TTB structure projection along a 001 direction. For a general formulation $A_2BC_2M_5X_{15}$ ($X = O, F$), large cations (e.g., Na^+, K^+, Sr^{2+}, Ba^{2+}, Pb^{2+}, La^{3+}, ...) occupy the pentagonal (A) and the square sites (B), small cations like Li^+ are in the triangular sites (C), and highly charged cations (e.g., Nb^{5+}, Ta^{5+}, ...) are in the octahedral M site.

The first compositions previously announced as relaxors concerned the $Ba_{2.5(1-x)}Sr_{2.5x}Nb_5O_{15}$ solid solution ($0.25 \leq x \leq 0.75$). In fact, the large (Ba^{2+}) and smaller (Sr^{2+}) cations must fill two large (A) crystallographic sites and one smaller (B) one. For the richest Ba compositions, a cationic order is probable as the largest sites are more numerous. In fact, the ferroelectric compositions corresponding to $0.25 \leq x < 0.60$ are indeed of classical type. In

TABLE 3
Comparative Values of x for the Same Shift of T_m ($\Delta T_m = 10$ K)

Substitution	Sites	Solid solutions	x
Homovalent	M	$Ba(Ti_{1-x}Zr_x)O_3$	0.35
	A and M	$Ba_{1-x}Ca_x(Ti_{1-x}Zr_x)O_3$	0.225
Heterovalent	A	$Ba_{1-x}K_{x/2}La_{x/2}TiO_3$	0.30
	A and M	$Ba_{1-x/2}\square_{x/2}(Ti_{1-x}Nb_x)O_3$	0.10
		$Ba_{1-x}K_x(Ti_{1-x}Nb_x)O_3$	0.125
	M and X	$Ba(Ti_{1-x}Li_x)O_{3-3x}F_{3x}$	0.15

TABLE 4
Comparative Values of ΔT_m for x Limit Value of Some Lead-Free Solid Solutions of Perovskite Type

Solid solutions	x limit value	ΔT_m[a] (K) for x limit value
$Ba(Ti_{1-x}Zr_x)O_3$	0.42	19
$Ba_{1-x}K_{x/2}La_{x/2}TiO_3$	0.30	9
$Ba_{1-x}La_{2x/3}\square_{x/3}TiO_3$	0.20	20
$Ba_{1-x}Bi_{2x/3}\square_{x/3}TiO_3$	0.15	36
$Ba_{1-x/2}\square_{x/2}(Ti_{1-x}Nb_x)O_3$	0.18	19
$Ba_{1-x}K_x(Ti_{1-x}Nb_x)O_3$	0.20	25
$Ba(Ti_{1-x}Li_x)O_{3-3x}F_{3x}$	0.16	12
PMN		15

[a] $\Delta T_m = T_m(10^5\ \text{Hz}) - T_m\ (10^2\ \text{Hz})$.

contrast, for the richest Sr compositions ($0.60 \leq x \leq 0.75$), the cationic disorder which occurs breaks the long-range order and generates a local polarization and thus a relaxor behavior (27–29).

Very recently, relaxor behavior was demonstrated in other compositions (Table 5). Of all the lead-free compounds studied, it is with a composition containing Bi^{3+}, another $6(sp)^2$ lone pair cation, that the highest value of T_m was obtained: T_m ($BaBiNb_5O_{15}$) = 319 K at 10^3 Hz. In addition, independently of the value of T_m, the two bismuth compositions allow the highest values of ΔT_m: $\Delta T_m = 80$ and 73 K for the potassium and the barium compounds respectively. Such a result is in good agreement with that obtained for lead-free compositions derived from $BaTiO_3$.

Some solid solutions situated between classical ferroelectric and relaxor ones have also been studied. Such is the case with $A_2B(Nb_{1-x}Ta_x)_5O_{15}$. The relaxor behavior occurs for

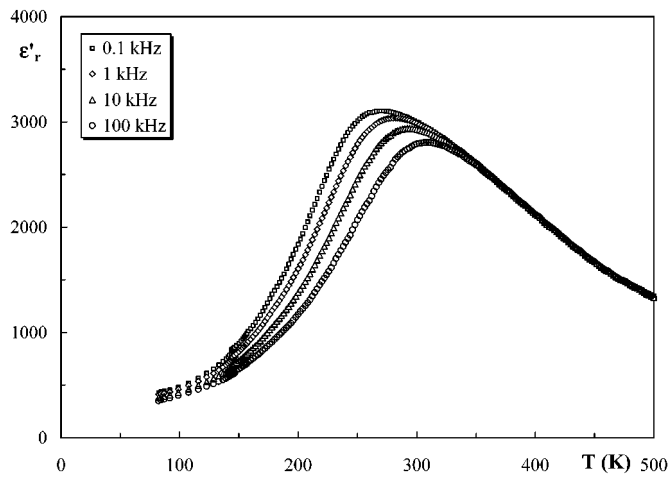

FIG. 4. Thermal variation of the real part of the permittivity ε'_r for a ceramic with composition $Ba_{0.85}Bi_{0.10}TiO_3$.

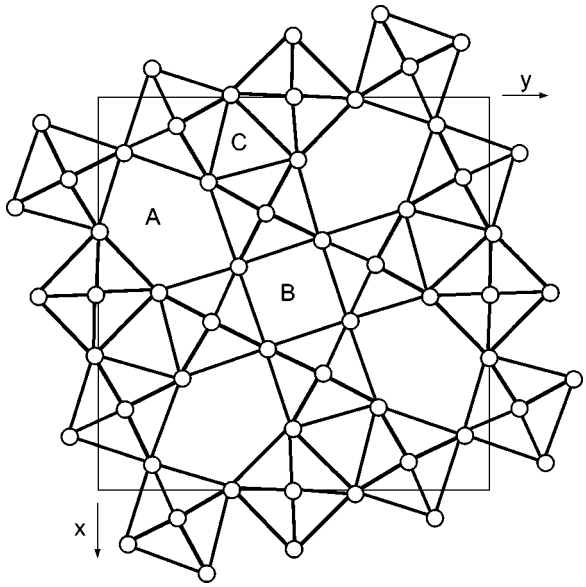

FIG. 5. Schematic projection of the TTB structure along the 4-fold c axis (A, B, and C correspond to cationic sites with 15, 12, and 9 coordination number).

the highest values of x. Figure 6 shows, as an example, the variations of T_C and T_m for ceramics with composition $Sr_2K(Nb_{1-x}Ta_x)_5O_{15}$. The replacement of very ferroelectrically active Nb^{5+} by the less active Ta^{5+} transforms the macroscopic polarization into a local one. This is also the case with the $Sr_2KNb_5O_{15}$–$SrK_2Nb_5O_{14}F$ and $Ba_2NaNb_5O_{15}$–$BaNa_2Nb_5O_{14}F$ systems; for compositions close to the oxide, the behavior is ferroelectric while it becomes relaxor when the fluorine rate and thus the sodium or potassium rate are sufficiently high (Fig. 7) (30). As for perovskites, relaxor, ferroelectric, and paraelectric behaviors also occur for some compositions, depending on the temperature. The frequency dependence of the permittivities of a ceramic with a composition $BaNa_2Nb_5O_{14}F$ clearly displays a frequency relaxation at 77 K, while it disappears at 300 K, i.e., for $T > T_m$ ($T_m = 140$ K at 10^3 Hz) (Fig. 8). The crystal structure determination of this compound is in good agreement with the dielectric properties, i.e., the A site is statistically occupied by equal quantities of Ba^{2+} and Na^+, thereby giving a cationic disorder in this A site while the B site is filled by Na^+ cations (31).

3b. Discussion

As for the perovskites, the relaxor effect appears in many TTB-type compounds when at least two ions occupy the same site. The coexistence of cations seems as favorable in the A site as in the M site. At least one cation ferroelectrically active in the octahedral site must be present.

TABLE 5
Some New Lead-Free TTB Relaxor Compositions

Relaxor compositions	T_m[a] (K) (at 10^3 Hz)	ΔT_m[a] (K) for x limit values
$K_2LaNb_5O_{15}$	165	22
$K_2BiNb_5O_{15}$	220	80
$BaLa\square Nb_5O_{15}$	203	55
$BaBi\square Nb_5O_{15}$	319	73
$BaLa_{2/3}\square_{1/3}NaNb_5O_{15}$	210	34
$BaLaNa(Nb_4Ti)O_{15}$	171	41
$BaLaK(Nb_4Ti)O_{15}$	146	13
$Sr_2NaTa_5O_{15}$	120	25
$Sr_2KTa_5O_{15}$	<80	*
$Ba_2NaTa_5O_{15}$	<80	*
$Ba_2KTa_5O_{15}$	<80	*
$SrK_2Nb_5O_{14}F$	112	16
$BaNa_2Nb_5O_{14}F$	140	17
$Sr_2Na(Nb_{1-x}Ta_x)_5O_{15}$ $(0.40 \le x \le 1)$	$222 \ge T_m \ge 120$	20 (0.40) to 25 (1)
$Sr_2K(Nb_{1-x}Ta_x)_5Nb_5O_{15}$ $(0.16 \le x \le 1)$	$263 \ge T_m \ge 80$	21 (0.16) to * (1)
$Ba_2Na(Nb_{1-x}Ta_x)_5O_{15}$ $(0.65 \le x \le 1)$	$260 \ge T_m \ge 80$	6 (0.65) to * (1)
$Ba_2K(Nb_{1-x}Ta_x)_5O_{15}$ $(0.35 \le x \le 1)$	$268 \ge T_m \ge 80$	16 (0.35) to * (1)
$Ba_{2-x}Na_{1+x}Nb_5O_{15-x}F_x$ $(0.31 \le x \le 1)$	$250 \ge T_m \ge 140$	40 (0.31) to 17 (1)
$Ba_2Na(Nb_{5-x}Ti_x)O_{15-x}F_x$ $(0.31 \le x \le 0.50)$	$265 \ge T_m \ge 168$	15 (0.31) to 30 (0.50)
$Sr_{2-x}K_{1+x}Nb_5O_{15-x}F_x$ $(0.20 \le x \le 1)$	$290 \ge T_m \ge 112$	15 (0.20) to 16 (1)

[a] $\Delta T_m = T_m$ (10^5 Hz) $- T_m$(10^2 Hz). *, unknown value.

The relaxor effect is mainly due to a cationic disorder in the A site, whatever the coupled substitution ensuring the electrical neutrality. This is the case with $BaLaNb_5O_{15}$ when Ba^{2+} and La^{3+} occupy only the A site.

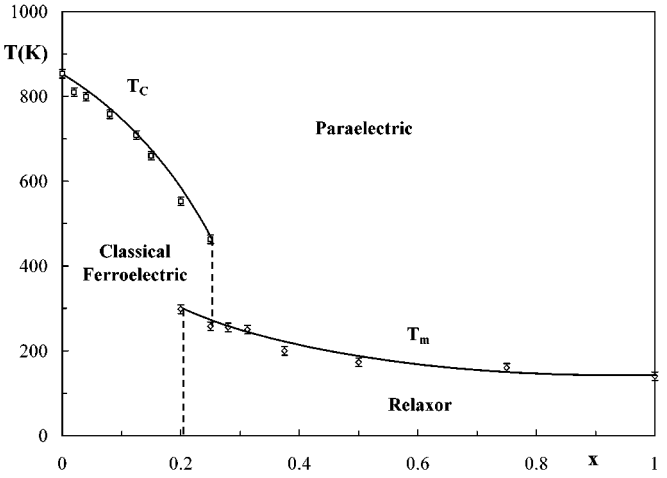

FIG. 7. Variation of transition temperatures with x for ceramics with composition $Ba_{2-x}Na_{1+x}Nb_5O_{15-x}F_x$ (30).

$Ba_2NaNb_5O_{15}$, in which the same two Ba^{2+} cations occupy the A site, is a classical ferroelectric. In contrast, $BaNa_2Nb_5O_{14}F$, in which the A site is half occupied by Ba^{2+} and Na^+, is a relaxor one. Moreover, the Ta–Nb substitution induces the disappearance of the classical ferroelectric effect and the appearance of the relaxor one. This results in a relaxor state as the long-range order is not induced by a local dipolar order. The higher the associated cationic order in the A and B sites, the higher the Ta–Nb substitution rate leading to relaxor behavior (Table 5); e.g. $x = 0.16$ for $Sr_2K(Nb_{1-x}Ta_x)_5O_{15}$ and $x = 0.65$ for $Ba_2Na(Nb_{1-x}Ta_x)_5O_{15}$. In fact there is no ambiguity regarding the disordered distribution of the two small Sr^{2+} cations and the single large K^+ one, nor regarding the

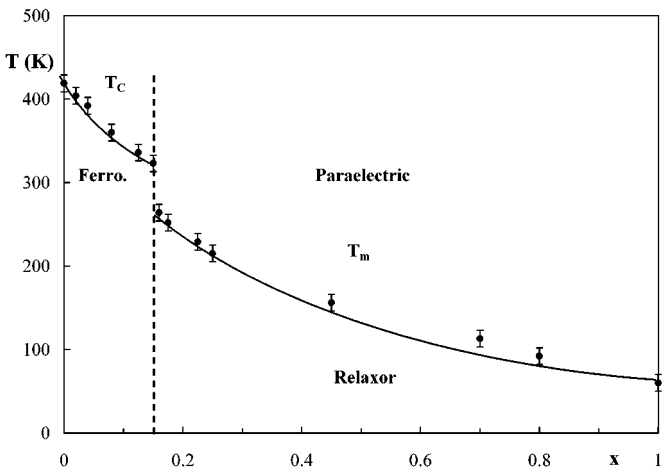

FIG. 6. Variation of transition temperatures with x for ceramics with composition $Sr_2K(Nb_{1-x}Ta_x)_5O_{15}$.

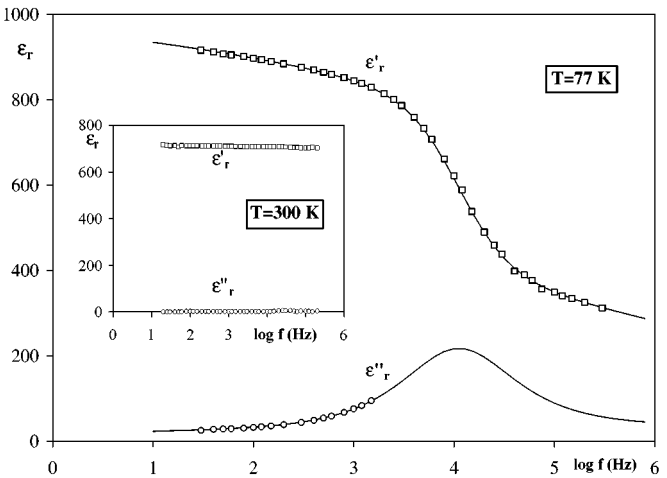

FIG. 8. Frequency dependencies of the permittivities ε'_r and ε''_r for a ceramic with composition $BaNa_2Nb_5O_{14}F$. The dashed line shows the fit of data according to the Cole–Cole model.

ordered distribution of the two large Ba^{2+} cations and the single small Na^{+} ones since both occur in two large A sites and in one smaller B one.

4. CONCLUSION

In each family investigated, i.e., perovskite or TTB-type, the relaxor behavior appears when at least two different cations occupy the same crystallographic site. This condition is necessary but not sufficient. The lack of relaxor effect in perovskite $BaMg_{1/3}Nb_{2/3}O_3$ is a good example. One of the M^{n+} cations in the octahedral site has to be ferroelectrically active (e.g., Ti^{4+}, Nb^{5+}, or Ta^{5+}). In any case, a local polarization leads to a relaxor effect while a macroscopic one gives a classical ferroelectric behavior.

Lead-free perovskites derived from $BaTiO_3$ are solid solutions. The only local polarization comes from dilution of the ferroelectric character. The relaxor effect is greater if the substitution affects the octahedral site. The higher the substitution rate, the greater the relaxor effect. For TTB-type compositions, the effect is due to either a cationic disorder in the A or B site or to a dilution of the ferroelectric character by cationic or anionic substitution, whatever the crystallographic site.

REFERENCES

1. L. E. Cross, *Ferroelectrics* **151,** 305–320 (1994).
2. K. Uchino, *Ferroelectrics* **151,** 321–330 (1994).
3. V. Hornebecq, C. Elissalde, F. Weill, A. Villesuzanne, M. Menetrier, and J. Ravez, *J. Appl. Crystallogr* **33,** 1037–1045 (2000).
4. G. Smolenski and A. Agranovskaya, *Sov. Phys. Solid State* **1,** 1429–1437 (1960).
5. B. Rolov, *Sov. Phys. Solid State* **6,** 1976–1979 (1965).
6. L. E. Cross, *Ferroelectrics* **76,** 241–267 (1987).
7. C. A. Randall and A. S. Bhalla, *Jpn J. Appl. Phys.* **29,** 327–333 (1990).
8. N. W. Thomas, *J. Phys. Chem. Solids* **51,** 1419–1431 (1990).
9. E. Husson, M. Chubb, and A. Morell, *Mater. Res. Bull.* **23,** 357–361 (1988).
10. N. De Mathan, Ph.D. thesis, Ecole Centrale de Paris, France, 1991.
11. H. D. Rosenfeld and E. Egami, *Ferroelectrics* **158,** 351–356 (1994).
12. H. Qian and L. A. Bursill, *Int. J. Mod. Phys. B* **10,** 2027–2047 (1996).
13. H. Qian, J. L. Peng, and L. A. Bursill, *Int. J. Mod. Phys. B* **7,** 4353–4369 (1993).
14. D. Viehland, M. Wuttig, and L. E. Cross, *Ferroelectrics* **120,** 71–77 (1991).
15. R. Pirc and R. Blinc, *Phys. Rev. B* **60**(19), 13470–13478 (1999).
16. V. Westphall, W. Kleeman, and M. D. Glinchuk, *Phys. Rev. Lett.* **68,** 847–850 (1992).
17. A. E. Glazounov, A. K. Tagantsev, and A. J. Bell, *Ferrroelectrics* **184,** 217–226 (1996).
18. I. W. Chen and Y. Wang, *Ferroelectrics* **206–207,** 245–263 (1998).
19. T. Egami, W. Dmowski, S. Teslic, P. K. Davies, I. W. Chen, and H. Chen, *Ferroelectrics* **206–207,** 231–244 (1998).
20. T. Egami, *Ferroelectrics* **222,** 163–170 (1999).
21. J. Ravez and A. Simon, *Eur. Phys. J. AP* **11,** 9–13 (2000).
22. J. Ravez and A. Simon, *Mater. Lett.* **36,** 81–84 (1998).
23. V. V. Lemanov, N. V. Zaitseva, E. P. Smirnova, and P. P. Syrnikov, *Ferroelectr. Lett.* **19,** 7–12 (1995).
24. J. Ravez and A. Simon, *Phys. Stat. Sol.* **159,** 517–522 (1997).
25. Ph. Sciau, Z. Lu, G. Galvarin, T. Roisnel, and J. Ravez, *Mater Res. Bull.* **28,** 1233–1239 (1993).
26. J. Suchanicz, *Ferroelectrics* **190,** 77–81 (1997).
27. P. B. Jamieson, S. C. Abrahams, and J. L. Bernstein, *J. Chem. Phys.* **48,** 5048–5057 (1968).
28. D. Viehland, S. Jang, and L. E. Cross, *Philos. Mag. B* **64,** 335–352 (1991).
29. F. Prokert, H. Ritter, and J. Ihringer, *Ferroelectr. Lett.* **24,** 1–7 (1998).
30. H. El Alaoui-Belghiti, A. Simon, M. Elaatmani, J. M. Reau, and J. Ravez, *Phys. Stat. Sol.* (*a*), in press.
31. R. Von Der Mühll and J. Ravez, *Bull. Soc. Fr. Mineral. Cristallogr.* **98,** 118–120 (1975).